Proc. Natl. Acad. Sci. USA
Vol. 96, pp. 6495–6500, May 1999
Physiology

Formation of heteromeric gap junction channels by connexins 40 and 43 in vascular smooth muscle cells

DING SHENG HE*, JEAN X. JIANG†, STEVEN M. TAFFET‡, AND JANIS M. BURT*§

*Department of Physiology, Arizona Health Sciences Center, University of Arizona, Tucson, AZ, 85724; †Department of Biochemistry, University of Texas Health Science Center, San Antonio, TX, 78284; and ‡Department of Microbiology and Immunology, State University of New York Health Science Center, Syracuse, NY 13210

Edited by Lily Yeh Jan, University of California, San Francisco, CA, and approved March 31, 1999 (received for review February 10, 1999)

ABSTRACT **Connexin (Cx) 43 and Cx40 are coexpressed in several tissues, including cardiac atrial and ventricular myocytes and vascular smooth muscle. It has been shown that these Cxs form homomeric/homotypic channels with distinct permeability and gating properties but do not form functional homomeric/heterotypic channels. If these Cxs were to form heteromeric channels, they could display functional properties not well predicted by the homomeric forms. We assessed this possibility by using A7r5 cells, an embryonic rat aortic smooth muscle cell line that coexpresses Cxs 43 and 40. Connexons (hemichannels), which were isolated from these cells by density centrifugation and immunoprecipitated with antibody against Cx43, contained Cx40. Similarly, antibody against Cx40 coimmunoprecipitated Cx43 from the same connexon fraction but only Cx40 from Cx (monomer) fractions. These results indicate that heteromeric connexons are formed by these Cxs in the A7r5 cells. The gap junction channels formed in the A7r5 cells display many unitary conductances distinct from homomeric/homotypic Cx43 or Cx40 channels. Voltage-dependent gating parameters in the A7r5 cells are also quite variable compared with cells that express only Cx40 or Cx43. These data indicate that Cxs 43 and 40 form functional heteromeric channels with unique gating and conductance properties.**

Gap junction channels connect the cytoplasms of adjacent cells and provide a pathway for intercellular diffusion of ions, second messenger molecules, and small metabolites. Functional gap junction channels are formed by connexins (Cxs), a gene family with at least 14 mammalian members that are distinguished from one another by their predicted molecular weights expressed in kilodaltons (e.g., Cx43, the 43-kDa connexin). Cxs oligomerize to form connexons (hemichannels), which are defined as homomeric when the six comprising Cxs are identical or heteromeric when two or more Cxs comprise the connexon. Connexons in adjacent cells join in the extracellular space to form the functional intercellular channel, which is defined as homotypic when the Cx composition of the contributing connexons is identical or heterotypic when different.

The ability of Cxs to form homomeric/heterotypic channels has been examined in the *Xenopus* oocyte and HeLa cell expression systems as well as in other settings (for review, see ref. 1). Homomeric Cx43 connexons successfully dock with homomeric connexons comprised of Cxs 30.3, 37, and 45 but not with Cxs 50, 40, 33, 32, 31.3, 31, or 26. Homomeric Cx40 connexons successfully dock with and form functional homomeric/heterotypic channels with Cxs 37 and 45 but not with Cxs 50, 46, 43, 32, 31.1, 31, or 26. Clearly, there are far more incompatible than compatible combinations.

The capacity of Cxs to form functional heteromeric connexons and channels has only recently received attention. Biochemical and structural tools have demonstrated the existence of heteromeric connexons comprised of Cxs 46 and 50 (2) and Cxs 32 and 26 (3). That these Cx pairs form functional heteromeric connexons recently has been demonstrated (4, 5), but formation of heteromeric channels by these Cx pairs has not been demonstrated. Based solely on functional data, it appears that Cxs 37 and 43 form heteromeric channels (6). The functional studies of heteromeric connexons and channels demonstrate that these structures display unique conductances, gating behaviors, or selectivities relative to the homomeric forms. There are no studies in which biochemical (or structural) and functional data are provided in support of formation of functional heteromeric channels by any pair of Cxs, certainly not Cx-pairs incapable of forming homomeric/heterotypic channels.

Coexpression of Cxs that fail to form homomeric/heterotypic channels occurs in many tissues and cell types including (tissue or cell type, expressed Cxs): keratinocytes, 43, 37, 31, 31.1, 26; testis, 43, 33; endothelial cells, 43, 40, 37; corneal epithelium, 43, 50; atrioventricular valves, 43, 50; atrial myocytes, 40, 43, 45; vascular smooth muscle, 40, 43; and thyroid follicular cells, 43, 32 (1, 7). In view of the changes in permeation and gating apparently induced by heteromerization, the implications of functional heteromers between Cxs incapable of forming functional homomeric/heterotypic channels could be profound. Thus, the goals of the present study are to determine whether Cxs 40 and 43 form heteromeric channels and, if so, to characterize the functional properties of those channels. We demonstrate that these Cxs form heteromeric channels with functional properties not well predicted by homomeric/homotypic Cx40 or Cx43 channels. Our results represent a demonstration of heteromeric channel formation and function in a mammalian cell line that naturally coexpresses the Cxs.

MATERIALS AND METHODS

Reagents. A7r5 cells were obtained from American Type Culture Collection. Tissue culture reagents were from GIBCO. Fetal bovine serum was obtained from HyClone or Intergen (Purchase, NY). [^{35}S]methionine (cell-labeling grade) was from New England Nuclear. Anti-Cx40 polyclonal antibody was from Chemicon. All other chemicals were obtained from either Sigma or Fisher Scientific.

Preparation and Immunoaffinity Purification of Anti-Cx43 Antibody. Bacterial fusion proteins containing glutathione *S*-transferase plus C-terminal portions of Cx43 (amino acids

The publication costs of this article were defrayed in part by page charge payment. This article must therefore be hereby marked "*advertisement*" in accordance with 18 U.S.C. §1734 solely to indicate this fact.

PNAS is available online at www.pnas.org.

This paper was submitted directly (Track II) to the *Proceedings* office.
Abbreviation: Cx, connexin.
§To whom reprint requests should be addressed at: Department of Physiology, Arizona Health Sciences Center, Room 4103, University of Arizona, 1501 North Campbell Avenue, Tucson, AZ 85724. e-mail: jburt@u.arizona.edu.

270–336) were generated by using the vector pGEX-1 (8). Overnight cultures were diluted 1/100 in fresh LB medium supplemented with ampicillin and were grown for 3 h before induction of fusion protein synthesis by the addition of isopropyl β-D-thiogalactopyranoside to a final concentration of 0.5 mM. After 4 h of induction, the cells were pelleted by centrifugation at 2,100 × *g* for 10 min. The pellet was resuspended in cold PBS, was sonicated with 1% Triton X-100 for 2 min on ice, and was centrifuged at 5,600 × *g* at 4°C for 10 min. The supernatant was passed through an affinity column of glutathione immobilized on Sepharose. The bound fusion protein was released with 5 mM glutathione. Ten-percent SDS/PAGE was used to separate full-length fusion protein from degradation products and then was stained with copper chloride (2), followed by excision from the gel. The gel strips were electroeluted in dialysis bags, and the eluted protein was concentrated in an Ultrafree-MC30,000 NMWL Filter Unit (Millipore). The purified full-length fusion protein was used to raise polyclonal antibodies in rabbits by Alpha Diagnostic (San Antonio, TX).

Metabolic Labeling and Crude Membrane Preparation. A7r5 cells were grown in culture medium (DMEM with 10% fetal bovine serum) on 100-mm culture plates until confluent. The confluent A7r5 cells were rinsed three times with medium deficient in methionine before the addition of 3 ml of ^{35}S-labeling medium (methionine-free DMEM with 5% dialyzed fetal calf serum, 20 μM methionine, and 1.5 mCi [^{35}S]methionine) for 3 h at 37°C. The metabolically labeled cells were lysed in lysis buffer (5 mM Tris/5 mM EDTA/EGTA, pH 8.0), and crude membranes were prepared by centrifugation (35,000 rpm, Beckman SW60Ti) for 30 min. The pellets were resuspended in "incubation buffer" (0.14 M NaCl/5.3 mM KCl/0.35 mM Na_2HPO_4/0.35 mM KH_2PO_4/0.8 mM $MgSO_4$/2.7 mM $CaCl_2$/20 mM Hepes, pH 7.5) and 10% Triton-X-100 and were incubated for 10 min at room temperature. Triton-solubilized specimens were separated by centrifugation (20,000 rpm, Beckman SW28 rotor, 30 min).

Sucrose Gradient Sedimentation Analysis. The detergent solubilized membranes were fractionated on a linear gradient of 5–20% sucrose (wt/vol at 20°C) (4 ml total) in the presence of the above-described incubation buffer and 0.5% Triton X-100. Centrifugation was performed in a Beckman SW60 Ti rotor at 49,000 rpm for 14 h at 4°C, after which, 300-μl fractions were collected. Cx43 monomers are known to migrate with a sedimentation coefficient of 5S whereas connexons migrate with a sedimentation coefficient of 9S. The 9S fraction has been demonstrated by electron microscopy to be highly enriched for connexons (9). Glutamate decarboxylase (EC 4.1.1.15; 310 kDa) or connexons composed of MP70 (Cx50) (2) were used as markers for the connexons with a sedimentation coefficient of 9S. Cxs, prepared by SDS-solubilization, were used as a marker for monomeric Cxs with a sedimentation coefficient of 5S. Ovine lens MP70, prepared by 8-Glu solubilization, was used as a marker for connexon pairs with a sedimentation coefficient of 16 S (2). Based on protein standards and calculations of the sucrose gradient conditions used in these experiments, the sedimentation coefficient 9S migration centered at fraction 12, 5S centered at fraction 5, and 16S centered at fraction 15.

Immunoprecipitation and SDS Gel Electrophoresis and Fluorography. Fractions from sucrose gradients were immunoprecipitated with either anti-Cx43 or anti-Cx40 antibody in the presence of immunoprecipitation buffer (0.1 M NaCl/0.02 M Na borate/15 mM EDTA/15 mM EGTA) supplemented with 0.5% Triton at 4°C for 16 h, and then, protein A-Sepharose beads were added for another 2 h. The beads were washed five times with immunoprecipitation buffer plus 0.5% BSA and 0.5% Triton X-100. The immunoprecipitated samples were isolated from the beads by boiling in SDS sample buffer for 5 min and were analyzed on 10% SDS/PAGE gels. Gels loaded with ^{35}S-labeled samples were processed for fluorography (2).

Cx40 Stable Transfectants. The clone for murine Cx40 was obtained from Klaus Willecke (Bonn University). A 1.1-kilobase fragment (10) was subcloned into the *Hin*dIII and *Eco*RI sites of pcDNA3 (Invitrogen), an expression vector that uses the cytomegalovirus promoter. Transfection into N2A cells (American Type Culture Collection) was accomplished by using Lipofectin (BRL). Transfected cells were plated by limiting dilution into 96-well plates and were selected by using 800 μg/ml G418 (BRL). Positive clones were determined by electrophysiologic analysis.

Electrophysiology. Confluent A7r5 or Rat-1 cells were trypsinized (0.25% trypsin in Ca-Mg free phosphate-buffered saline) and were replated at low density on glass coverslips. After a 30-min incubation at 37°C, the cells were subsequently maintained and used for electrophysiologic experiments at room temperature. Single-channel data were typically obtained within 2.5 h of plating; voltage-dependent gating data were obtained within 4–5 h of plating. N2A-Cx40 cells were plated at low density 24 h before electrophysiologic study. For all cell types, coverslips with attached cells were mounted in an experimental chamber, and the cells were bathed in a solution containing (in mM) 142.5 NaCl, 4 KCl, 1 $MgCl_2$, 0.9 NaH_2PO_4, 5 Dextrose, 2 Na-Pyruvate, 10 Hepes, 15 CsCl, 10 TeaCl, and 1 $BaCl_2$.

Dual whole-cell voltage clamp was carried out as reported (11, 12). Electrodes (5–10 megaohms) were fabricated from 1.2-mm filament glass (AM Systems, Everett, WA) on a Sutter Instruments puller (Novato, CA) and were filled with (in mM) 67.8 CsCl, 67.8 KGlu, 10 TeaCl, 0.5 $CaCl_2$, 3 $MgCl_2$, 5 Dextrose, 10 Hepes, 10 EGTA, 5 Na_2ATP, and 6.7 Na-creatine phosphate. After the dual whole-cell voltage clamp configuration was achieved, both cells were held at 0 mV and were alternately stepped to −10 mV to determine macroscopic junctional conductance (g_j). Single-channel events were studied in cell pairs with one or a few functional channels. No uncoupling agents such as halothane or heptanol were used in our studies because preliminary data indicate that channels comprised of Cx40, Cx43, or Cx40&43 display different sensitivities to these agents. Voltage-dependent gating was evaluated in cell pairs in which g_j was <7 nS.

Channel events typically were obtained with a transjunctional driving force of 40 mV, although some records were obtained with larger driving forces. Current data were digitized (Neurocorder, model DR 484, Neuro Data Instruments, New York) and stored on videotape. Desired segments of records were filtered (8-pole Bessel, 50 Hz) and acquired (Data Translation, Marlboro, MA) for computerized single-channel analysis by using the software of Ramanan, Brink, and colleagues (13, 14).

Voltage-dependent gating parameters were determined as follows. From a holding potential of 0 mV, one cell of a pair was stepped to +40 mV for 10–12 s, was returned to 0 mV for ≥12 s, and was stepped to −40 mV for 10–12 s. In an independent series of experiments, these step durations were found sufficient for steady state voltage-dependent changes to occur and similarly for channel recovery to occur. This pulsing protocol was repeated such that ± 40, ± 60, ± 80, ± 100, (± 120), and, finally, ± 20 mV were examined. Data from each cell pair were plotted (normalized conductance vs. transjunctional voltage) and dependence of conductance on positive and negative voltage was determined [Boltzmann fit (15)]. The Boltzmann parameters corresponding to V_0, G_{min}, and z for each cell type were calculated (expressed as mean ± SD) and were compared by using the Wilcoxon-Mann-Whitney test (a nonparametric two-sample ranked sums test). Differences were assumed significant when $P < 0.05$.

RESULTS

To determine whether heteromeric connexons were formed in A7r5 cells, ^{35}S-methionione metabolically labeled crude membranes solubilized by Triton-X-100 were centrifuged through 5–20% sucrose gradients. The resulting fractions were immunoprecipitated under nondenaturing conditions with affinity purified anti-Cx43 antibody, and the immunoprecipitated samples were resolved by SDS/PAGE and fluorography. As shown in Fig. 1*A*, Cx43 concentrated into two major peaks centered at fractions 5 and 12. By comparison, samples at fraction 5 should enrich monomeric Cxs, and those at fraction 12 should enrich connexons (2, 9). In addition to Cx43, there is an extra band with the same mobility as Cx40 in the connexon-rich fractions (fraction 11–12). To confirm that Cx40 directly associates with Cx43, connexon-rich fraction 12 was immunoprecipitated with Cx40 antibody and was resolved on SDS/PAGE (Fig. 1*B*). Anti-Cx40 antibody coimmunoprecipitated both Cx40 and Cx43 from connexon-rich fraction 12. To control for nonspecific or cross reactions of antibodies, monomeric-Cx rich fraction 5 was immunoprecipitated with Cx40 antibody, and only a single Cx40 band was detected. Immunoprecipitation by preimmune antibody did not resolve any protein bands. Together, the results show that Cx40 and Cx43 can be coimmunoprecipitated from connexon-rich samples by either Cx43 or Cx40 antibody, confirming that single connexons were composed of both Cxs. These data provide biochemical evidence that Cx43 and Cx40 form heteromeric connexons in A7r5 cells.

To determine whether these heteromeric connexons assemble into functional intercellular channels, we examined single-channel event amplitudes and characterized voltage-dependent gating behavior. Single-channel events derived from multiple pairs of A7r5 cells revealed channels of diverse amplitudes. Openings from the zero transjunctional current level included events with the following amplitudes: 170, 160, 144, 135, 120, 100, 95, 63, and 55 pS. In multichannel records, a variety of transition amplitudes was observed in the A7r5 cells (Fig. 2*A1* and *A2*) that were not evident in the Rat-1 (Fig. 2*B*) or N2A-Cx40 (Fig. 2*C*) cells. In some A7r5-pairs, most of the transitions had amplitudes of <100 pS (Fig. 2*A1*) whereas,

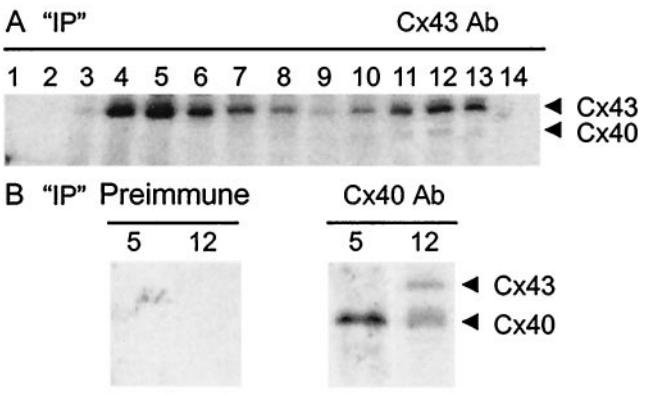

FIG. 1. Cxs 40 and 43 coimmunoprecipitated from connexon-enriched fractions. Crude membranes isolated from A7r5 cells after [^{35}S]methionine labeling were solubilized in Triton X-100 and were fractionated on a 5–20% linear sucrose gradient (see text). Individual gradient fractions were immunoprecipitated and analyzed by SDS/PAGE and fluorography. In *A*, each fraction was immunoprecipitated with affinity-purified anti-Cx43 antibody. A second band with the same mobility as Cx40 is observed in fractions enriched for connexons (e.g., fraction 12). In *B*, fractions 5 and 12 were immunoprecipitated with preimmune serum or Cx40 antibody. No bands were detected with preimmune serum. A second band with the same mobility as Cx43 is observed in the connexon-enriched fraction 12 but not in the Cx-enriched fraction 5.

in other pairs, larger transition amplitudes predominated (Fig. 2*A2*). The variability in transition amplitude is apparent in the all-points histogram as broad peaks that fail to start and stop at baseline and whose separations do not correspond to actual event amplitudes. These results from A7r5 cells are strikingly different from those obtained from Rat-1 cells, which express only Cx43, and from N2A-Cx40 cells. In Rat-1 cells, Cx43 displayed main and residual state conductances of 89 and 34 pS, respectively. In N2A-Cx40 cells, Cx40 channels exhibited main and residual state conductances of 166 and 26 pS. For both Cx43 and Cx40 channels, transitions between the main and residual states predominated; complete channel closure occurred extremely rarely. Thus, records from Rat-1 cells displayed mainly 55 and 35 pS transitions (Fig. 2*B*) whereas 140-pS transitions predominated in the N2A-Cx40 records (Fig. 2*C*). The uniformity of event amplitudes in the homomeric/homotypic setting is evident in the all-points histograms as narrow, well defined peaks that start and end at baseline and whose separations correspond to actual event amplitudes. The differences between A7r5 and either the Rat-1 or N2A-Cx40 cells strongly suggest the presence of functional heteromeric channels in the A7r5 cells.

Voltage-dependent gating of gap junction conductance was also quite variable in the A7r5 cells. In Fig. 3*A*, the normalized conductance (G_{ss}/G_{inst}) vs. transjunctional voltage data obtained from 10 A7r5 cell pairs are shown. In keeping with the diversity of channel types displayed by pairs of A7r5 cells, we also observed a variety of voltage-dependent gating behaviors. In contrast to this diversity, data from seven pairs of Rat-1 cells (Fig. 3*B*) and six pairs of N2A-Cx40 cells were much more homogeneous. Macroscopic junctional conductance ranged between 1 and 7 nS for all cell pairs, and mean conductances did not differ: 2.5 ± 1.7, 2.5 ± 1.0, and 2.7 ± 2.2 nS for the A7r5, Rat-1, and N2A-Cx40 cells, respectively. Data from each cell pair were fit with the Boltzmann equation to determine V_0, G_{min}, and z. As expected from the diversity of curves in Fig. 3*A*, the standard deviation about the mean for these parameters in the A7r5 cells was quite large compared with that obtained in the Rat-1 or N2A-Cx40 cells. The positive voltage at which current was half-maximal (V_0) was 72 ± 16 mV for A7r5 cells vs. 65 ± 2.7 mV for Rat-1 and 47 ± 6 mV for the N2A-Cx40 cells. The residual conductance at high transjunctional voltage (G_{min}) was 0.4 ± 0.22 in the A7r5 cells vs. 0.33 ± 0.05 for Rat-1 and 0.22 ± 0.03 for N2A Cx40 cells. The gating charge (z) was 1.9 ± 0.84 for A7r5 cells vs. 6.2 ± 2.8 for Rat-1 cells and 3.6 ± 1.6 for the N2A-Cx40 cells. V_0 and z values for the A7r5 cells differed from those obtained in the Rat-1 and N2A-Cx40 cells at the $P < 0.02$ level (Wilcoxon-Mann-Whitney test).

DISCUSSION

Using a combination of biochemical and electrophysiologic approaches, we demonstrate here that Cxs 40 and 43 form heteromeric channels in A7r5 cells. Cxs 40 and 43 were coimmunoprecipitated with either of the two specific antibodies from the sucrose gradient fraction enriched for connexons. Each antibody immunoprecipitated only its specific Cx after denaturation in SDS. These results strongly suggest the formation of Cx40/Cx43 heteromeric connexons in these cells. That these heteromeric connexons assemble to form functional channels is supported by three lines of electrophysiologic data. First, channel amplitudes not observed in the homomeric/homotypic settings predominated in the A7r5 cells. Second, voltage-dependent gating parameters were not well predicted by either Cx in their homomeric/homotypic forms. Third, in a previous study (12), it was found that the permeation characteristics of gap junctions formed by A7r5 cells were distinct from those of either Cx40 or Cx43. Thus, current and previous electrophysiologic data, in combination with our biochemical data, indicate that, despite their failure to form

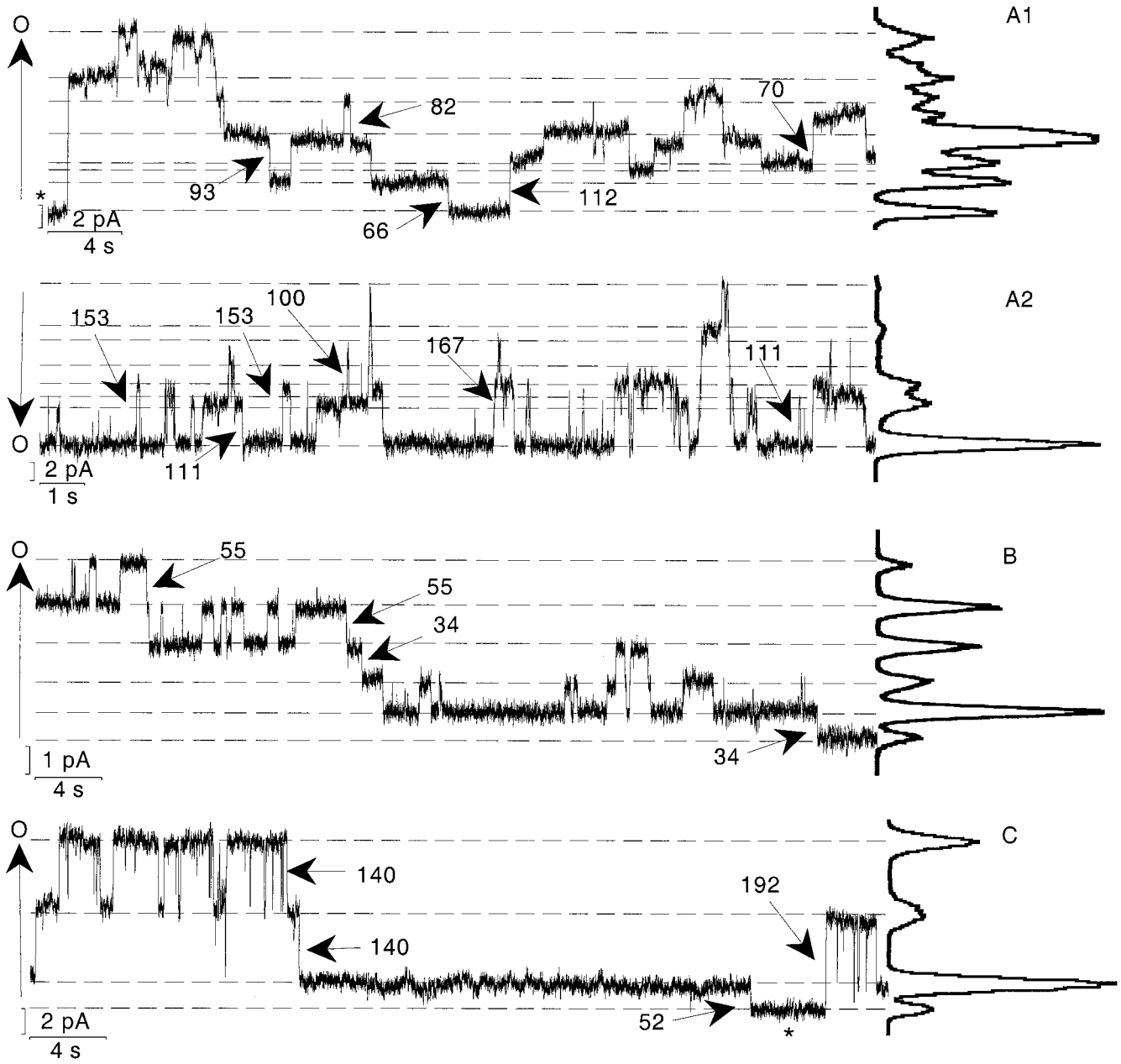

FIG. 2. Multichannel records obtained from A7r5 (*A1* and *A2*), Rat-1 (*B*), or N2A-Cx40 (*C*) cells. The A7r5 cells display event amplitudes not observed in the Rat-1 or N2A-Cx40 cells. In the all-points histograms for the Rat-1 and N2A cells, peaks are narrow, they begin and end at baseline, and their separations correspond to actual event amplitudes. In the all-points histograms for the A7r5 cells, peaks are broad, they do not begin and end at baseline, and peak separations do not correspond to actual event amplitudes. Transjunctional voltage was 40 mV throughout the A7r5 and N2A-Cx40 records except at the asterisks (in *A1* and *C*), where it was 0 mV. Transjunctional voltage was 30 mV throughout the Rat-1 record.

functional heterotypic channels, Cxs 40 and 43 form heteromeric channels with unique functional properties.

The single-channel properties of Cx43 homomeric/homotypic channels have been examined in numerous cell types, including (noninclusive) astrocytes (16), WB cells (17), leptomeningeal cells (18), fibroblasts (19), corpus cavernosum smooth muscle (20), ventricular myocytes (21, 22), and lens epithelium (23), and in Cx43 transfected neuroblastoma (24), HeLa (25), and hepatoma (26) cells. Collectively, these studies demonstrate that Cx43 channels exhibit at least one closed state and two distinct open states, referred to as the main and residual states. Transitions between the closed and residual states and between the closed and main states produce events of ≈30- and 95-pS amplitude, respectively. Because channel closure is rare (22), the most commonly observed transition, ≈65 pS, is between the main and residual states. The actual amplitudes of these transitions depend on the composition of the patch pipette solution (22). With a Cs-Aspartate (110 mM) solution, main and residual state conductances for Cx43 channels are 61 and 12 pS, respectively, whereas, with KCl (110 mM), these values are 96 and 23 pS. The relative frequency of ≈65-pS events is enhanced when phosphatase inhibitors are included in the patch pipet. The relative frequency of 95pS events (transitions between the main and closed states) is enhanced when activators of phosphatases are included. The consistent observation of ≈30-, 65-, and 95-pS events across multiple cell types and treatment conditions indicates that any cell-specific regulation of Cx43 channel conductances is likely encompassed by these observations.

The behavior of Cx40 homomeric/homotypic channels has been examined in HeLa (15, 25), neuroblastoma (27), and choriocarcinoma (28) cells. Cx40 channels display main and

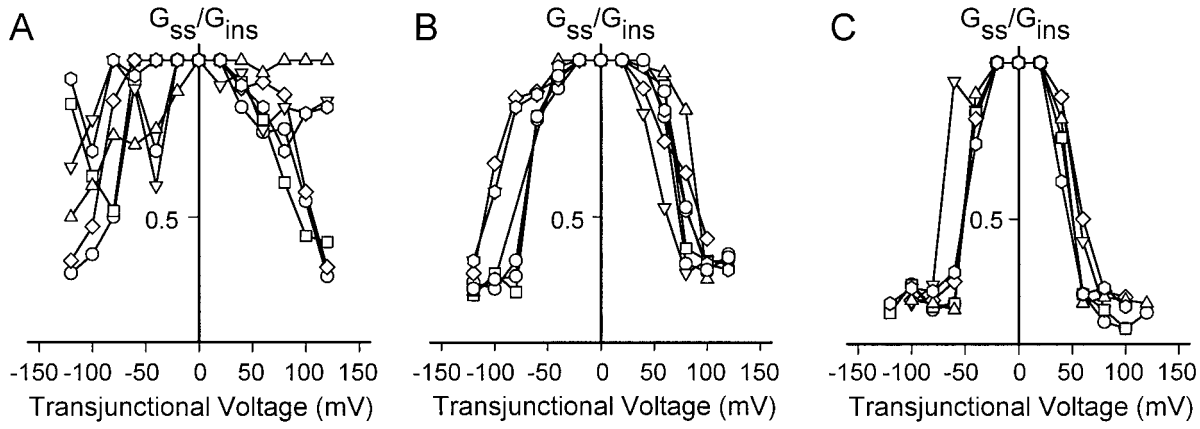

FIG. 3. Voltage-dependent gating of gap junction channels in A7r5 cells (*A*), Rat-1 cells (*B*), and N2A-Cx40 cells (*C*). Normalized junctional conductance [steady state relative to instantaneous (G_{ss}/G_{inst})] is plotted as a function of transjunctional voltage for 10 A7r5, 7 Rat-1, and 6 N2A-Cx40 cell pairs. Note the uniformity of responses to voltage in the Rat-1 and N2A cells compared with the diversity observed in the A7r5 cells.

residual state conductances of 162 and 28 pS with K-Aspartate (120 mM) pipette solution (15). Although Cx40 appears to be phosphorylated (25), it is not clear what effect, if any, phosphorylation has on channel behavior.

Our measurements of Cx40 channels in N2A cells and of Cx43 channels in Rat-1 cells are consistent with the data discussed above. We observed main and residual state conductances for Cx43 of 89 and 34 pS and for Cx40 of 166 and 26 pS. In the A7r5 cells, a diversity of transition amplitudes was observed, most of which are not observed in the homomeric/homotypic setting. In view of the large database available for behavior of the homomeric/homotypic channels formed by these Cxs (discussed above), it seems highly unlikely that the unique transition amplitudes observed in A7r5 cells result from cell-specific regulation of the homomeric/homotypic forms. Instead, the data strongly suggest that Cxs 40 and 43 form functional heteromeric channels that display conductances distinct from the homomeric/homotypic forms.

Cxs 40 and 43, in their homomeric/homotypic forms, display unique voltage-dependent gating behaviors. For Cx40, V_0, G_{min}, and z are ≈47 mV, 0.24, and 6, respectively (see ref. 28 for review). For Cx43, V_0, G_{min}, and z values are ≈59 mV, 0.16 and 2.3, respectively (22). Comparable values for Cx40 and Cx43 were obtained herein. The A7r5 cells displayed V_0, G_{min}, and z values of ≈72 mV, 0.4 and 1.9, respectively. The variability in the A7r5 cell measurements (Fig. 3) was dramatically higher than observed in the homomeric/homotypic settings. This high variability strongly supports formation of heteromeric channels by these Cxs and suggests (*i*) that heteromeric channels display unique gating properties and (*ii*) that the number of channels underlying macroscopic conductances of 2–3 nS, ≈20–30 if open probability is close to 1, is insufficient to adequately sample the possible channel mixture (see below). That heteromeric channels display alterations in their voltage-dependent gating behavior may suggest that other types of gating also will differ.

In a previous study, the macroscopic permeability of the junctions formed by A7r5 cells was determined (12). In the presence of serum, the junctions were permeated (nearly) equally well by small anions and cations but poorly by large ions of either charge. In reduced serum, the junctions were well permeated by large and small anions and cations, and fluorescent tracers diffused nearly five-fold better. Cx43 expression levels were comparable in the two conditions, but Cx40 expression was dramatically higher in the presence of serum (D. T. Kurjiaka, A. M. Fletcher, and J.M.B., unpublished observations). These results are difficult to reconcile with expression of only homomeric/homotypic Cx40 and Cx43 channels (22, 24, 27) but are easy to reconcile if heteromers of these Cxs display unique permeation properties. In view of the data supporting heteromeric channel formation presented here, it seems likely that the unique macroscopic permeability patterns observed in A7r5 cells reflect the contribution of heteromeric channels. The results suggest a cellular strategy for independent regulation of chemical and electrical communication that could be important to growth control and hypertrophy in excitable cells, where loss of electrical communication would be detrimental to survival of the organism.

The number of channel types that could be formed by Cxs 40 and 43 in a heteromeric setting is 194 (6) because the homomeric/heterotypic forms are not functional. If Cx40 and Cx43 each constitutes 50% of the total Cx pool, and if formation of the 194 possible channel types occurs randomly, then the chances of observing a homomeric/homotypic channel would be ≈0.024%. If Cx40 were twice as prevalent as Cx43 (i.e., if Cx40 represents 66% of the total Cx pool), the incidence of homomeric/homotypic Cx43 channels would decrease to ≈0.00019%, a ≈130-fold decrease relative to equal expression levels. In contrast, the incidence of Cx40 homomeric/homotypic channels would increase to ≈0.77%, a ≈32-fold increase. If only homomeric/homotypic channels formed, channel incidence would parallel expression levels (i.e., a 66:33 expression ratio would produce 66:33 incidence of the corresponding channel types). Clearly, small changes in the expression ratio could have profound effects on the channel population in the heteromeric setting. Because conductance, gating, and permeation properties of the heteromeric channels appear to differ significantly from the homomeric/homotypic forms, small changes in expression would be expected to dramatically alter intercellular communication.

It is not clear how many heteromeric channel types are allowed, but the variability in gating behavior when ≈30 channels are contributing suggests that there are many. The rules governing heterotypic and heteromeric channel formation among Cxs are not known. The demonstration that two Cxs incompatible for docking can form heteromeric channels indicates that docking may in part be determined by subunit interactions within a connexon. This conclusion is supported by studies of chimeric Cxs. Haubrich *et al.* (29), working with chimera of Cx40 and 43, concluded that an intracellular domain (the C terminus) was a critical determinant of interactions in the extracellular domain. Our data, which indicate heteromeric channel formation by Cxs 40 and 43, further support subunit interactions as an important determinant of docking as well as channel function. Because coexpression of Cxs incapable of homomeric/heterotypic interaction is com-

mon, the importance of defining the rules for channel assembly is increasingly apparent. If all of these incompatible Cxs were able to form heteromeric channels with unique functional properties, cells and tissues would be able to exploit a greater dynamic range of function not available if only homomeric/homotypic channels were formed.

Expression of Cxs 40 and 43 is dynamically regulated in cells of the cardiovascular system. Disease processes that result in cell injury and proliferation, such as hypertension, atherosclerosis and ischemia (30–33) alter expression levels. As described above, the composition of the heteromeric channel is expected to be extremely sensitive to the expression ratio of the contributing Cxs. Thus, these changes in expression pattern could significantly alter intercellular communication. In this context, our observations offer a mechanistic basis for the predisposition to arrhythmias observed in Cx40 "knockout" animals. These animals retain Cx43 expression and conduct action potentials with only modest delay. However, the animals are predisposed to arrhythmias (34, 35). Our results suggest that the unique conductance, gating, and permeation properties of heteromeric channels may be crucial to normal rhythmicity as well as providing a mechanism for independent control of chemical vs. electrical communication.

This work was supported by National Institutes of Health (Public Health Service) Grants HL58732 and HL07249–23 to J.M.B., EY12085 to J.X.J., and HL39707 to S.M.T.

1. White, T. W. & Bruzzone, R. (1996) *J. Bioenerg. Biomembr.* **28,** 339–350.
2. Jiang, J. X. & Goodenough, D. A. (1996) *Proc. Natl. Acad. Sci. USA* **93,** 1287–1291.
3. Stauffer, K. A. (1995) *J. Biol. Chem.* **270,** 6768–6772.
4. Bevans, C. G., Kordel, M., Rhee, S. K. & Harris, A. L. (1998) *J. Biol. Chem.* **273,** 2808–2816.
5. Ebihara, L., Xu, X., Oberti, C., Beyer, E. C. & Berthoud, V. M. (1999) *Biophys. J.* **76,** 198–206.
6. Brink, P. R., Cronin, K., Banach, K., Peterson, E., Westphale, E. M., Seul, K. H., Ramanan, S. V. & Beyer, E. C. (1997) *Am. J. Physiol.* **173,** C1386–C1396.
7. Little, T. L., Beyer, E. C. & Duling, B. R. (1995) *Am. J. Physiol.* **268,** H729–H739.
8. Smith, D. B. & Johnson, K. S. (1988) *Gene* **67,** 31–40.
9. Kistler, J., Bond, J., Donaldson, P. & Engel, A. (1993) *J. Struct. Biol.* **110,** 28–38.
10. Hennemann, H., Suchyna, T., Lichtenberg-Frate, H., Jungbluth, S., Dahl, E., Schwarz, J., Nicholson, B. J. & Willecke, K. (1992) *J. Cell Biol.* **117,** 1299–1310.
11. He, D. S. & Burt, J. M. (1998) in *Gap Junctions*, ed. Werner, R. (IOS, Amsterdam), pp 40–44.
12. Kurjiaka, D. T., Steele, T. D., Olsen, M. V. & Burt, J. M. (1998) *Am. J. Physiol.* **275,** C1674–C1682.
13. Manivannan, K., Ramanan, S. V., Mathias, R. T. & Brink, P. R. (1992) *Biophys. J.* **61,** 216–227.
14. Ramanan, S. V. & Brink, P. R. (1993) *Biophys. J.* **65,** 1387–1395.
15. Bukauskas, F. F., Elfgang, C., Willecke, K. & Weingart, R. (1995) *Biophys. J.* **68,** 2289–2298.
16. Dermietzel, R., Hertzberg, E. L., Kessler, J. A. & Spray, D. C. (1991) *J. Neurosci.* **11,** 1421–1432.
17. Spray, D. C., Chanson, M., Moreno, A. P., Dermietzel, R. & Meda, P. (1991) *Am. J. Physiol.* **26,** C513–C527.
18. Spray, D. C., Moreno, A. P., Kessler, J. A. & Dermietzel, R. (1991) *Brain Res.* **568,** 1–13.
19. Goldberg, G. S., Martyn, K. D. & Lau, A. F. (1994) *Mol. Carcinog.* **11,** 106–114.
20. Moreno, A. P., Campos de Carvalho, A. C., Christ, G., Melman, A. & Spray, D. C. (1993) *Am. J. Physiol.* **264,** C80–C92.
21. Burt, J. M. & Spray, D. C. (1988) *Proc. Natl. Acad. Sci. USA* **85,** 3431–3434.
22. Valiunas, V., Bukauskas, F. & Weingart, R. (1997) *Circ. Res.* **80,** 708–719.
23. Donaldson, P. J., Roos, M., Evans, C., Beyer, E. & Kistler, J. (1994) *Invest. Ophthalmol. Visual Sci.* **35,** 3422–3428.
24. Wang, H.-Z. & Veenstra, R. D. (1997) *J. Gen. Physiol.* **109,** 491–507.
25. Traub, O., Eckert, R., Lichtenberg-Frate, H., Elfang, C., Bastide, B., Scheidtmann, K. H., Hulser, D. F. & Willecke, K. (1994) *Eur. J. Cell Biol.* **64,** 101–112.
26. Moreno, A. P., Saez, J. C., Fishman, G. I. & Spray, D. C. (1994) *Circ. Res.* **74,** 1050–1057.
27. Beblo, D. A. & Veenstra, R. D. (1997) *J. Gen. Physiol.* **109,** 509–522.
28. Zhang, J.-T., Chen, M., Foote, C. I. & Nicholson, B. J. (1996) *Mol. Biol. Cell* **7,** 471–482.
29. Haubrich, S., Schwarz, H. J., Bukauskas, F., Lichtenberg-Frate, H., Traub, O., Weingart R. & Willecke, K. (1996) *Mol. Biol. Cell* **7,** 1995–2006.
30. Gabriels, J. E. & Paul, D. L. (1998) *Circ. Res.* **83,** 636–643.
31. Haefliger, J. A., Castillo, E., Waeber, G., Bergonzelli, G. E., Aubert, J. F., Sutter, E., Nicod, P., Waeber, B. & Meda, P. (1997) *Circulation* **95,** 1007–1014.
32. Blackburn, J. P., Peters, N. S., Yeh, H.-I., Rothery, S., Green, C. R. & Severs, N. J. (1995) *Arterioscler. Thromb. Vasc. Biol.* **15,** 1219–1228.
33. Polacek, D., Lal, R., Volin, M., V. & Davies, P. F. (1993) *Am. J. Pathol.* **142,** 593–606.
34. Simon, A. M., Goodenough, D. A. & Paul, D. L. (1998) *Curr. Biol.* **8,** 295–298.
35. Kirchhoff, S., Nelles, E., Hagendorff, A., Kruger, O., Traub, O. & Willecke, K. (1998) *Curr. Biol.* **8,** 299–301.